62185-92-6; $(Mo_6Br_8)Br_4(PPr_3\text{-}n)_2$, 62185-93-7; $(Mo_6Br_8)Br_4(PBu_3\text{-}n)_2$, 68813-07-0; $(Mo_6Br_8)Br_4$(dppe), 68757-62-0; $(Mo_6I_8)I_4$, 12175-58-5; $(Bu_4N)_2Mo_4I_{11}$, 68024-65-7; $(Nb_6Cl_{12})Cl_2(H_2O)_4\cdot 4H_2O$, 12766-39-1; $(Et_4N)_3[(Nb_6Cl_{12})Cl_6]$, 12128-45-9; $(Bu_4N)_2[(Nb_6Cl_{12})Br_6]$, 68867-04-9; $(Nb_6Cl_{12})Cl_2(PPr_3\text{-}n)_4$, 68813-06-9; $(Nb_6Cl_{12})Cl_2(Me_2SO)_4$, 12335-06-7; $(Ta_6Cl_{12})Cl_2(H_2O)_4\cdot 4H_2O$, 51269-64-8; $(Et_4N)_2[(Ta_6Cl_{12})Cl_6]$, 12556-09-1; $(Bu_4N)_2[(Ta_6Cl_{12})Br_6]$, 68758-52-1.

References and Notes

(1) (a) Part 21: V. Srinivasan, E. I. Stiefel, A. Elsberry, and R. A. Walton, submitted for publication. (b) Part 20: V. Srinivasan and R. A. Walton, *Inorg. Chim. Acta*, **25**, L85 (1977).
(2) R. A. Walton, *Coord. Chem. Rev.*, **21**, 63 (1976).
(3) V. I. Nefedov, *J. Electron Spectrosc. Relat. Phenom.*, **12**, 459 (1977).
(4) D. G. Tisley and R. A. Walton, *Inorg. Chem.*, **12**, 373 (1973).
(5) D. G. Tisley and R. A. Walton, *J. Inorg. Nucl. Chem.*, **35**, 1905 (1973).
(6) A. D. Hamer and R. A. Walton, *Inorg. Chem.*, **13**, 1446 (1974).
(7) J. R. Ebner, D. L. McFadden, D. R. Tyler, and R. A. Walton, *Inorg. Chem.*, **15**, 3014 (1976).
(8) A. D. Hamer, D. G. Tisley, and R. A. Walton, *J. Chem. Soc., Dalton Trans.*, 116 (1973).
(9) H. D. Glicksman and R. A. Walton, *Inorg. Chim. Acta*, in press.
(10) J. R. Ebner, D. L. McFadden, and R. A. Walton, *J. Solid State Chem.*, **17**, 447 (1976).
(11) H. D. Glicksman and R. A. Walton, *Inorg. Chim. Acta*, **19**, 91 (1976).
(12) For a preliminary report on the Br 3p spectra of $(Mo_6Br_8)Br_4$ and its derivatives see S. A. Best, T. J. Smith, and R. A. Walton, *Inorg. Chim. Acta*, **21**, L21 (1977).
(13) W. L. Jolly, "The Synthesis and Characterization of Inorganic Compounds", Prentice-Hall, Englewood Cliffs, NJ, 1970, p 456.
(14) J. C. Sheldon, *J. Chem. Soc.*, 1007 (1960).
(15) H. D. Glicksman and R. A. Walton, *Inorg. Chem.*, **17**, 3197 (1978).
(16) B. G. Hughes, J. L. Meyer, P. B. Fleming, and R. E. McCarley, *Inorg. Chem.*, **9**, 1343 (1970).
(17) F. W. Koknat, J. A. Parsons, and A. Vonguusharintra, *Inorg. Chem.*, **13**, 1699 (1974).
(18) R. A. Field and D. L. Kepert, *J. Less-Common Met.*, **13**, 378 (1967).
(19) R. A. Mackay and R. F. Schneider, *Inorg. Chem.*, **6**, 549 (1967).
(20) A. D. Hamer, D. G. Tisley, and R. A. Walton, *J. Inorg. Nucl. Chem.*, **36**, 1771 (1974).
(21) R. A. Walton in "Proceedings of the Climax Second International Conference on the Chemistry and Uses of Molybdenum", P. C. H. Mitchell, Ed., Climax Molybdenum Co. Ltd., London, 1976, p 34; see also, *J. Less-Common Met.*, **54**, 71 (1977).
(22) G. E. McGuire, G. K. Schweitzer, and T. A. Carlson, *Inorg. Chem.*, **12**, 2450 (1973).
(23) M. K. Bahl, *J. Phys. Chem. Solids*, **36**, 485 (1975).
(24) Data from ref 6 has been corrected by +1.0 eV to make the referencing procedure compatible with that used in the present study.
(25) D. L. Kepert, "The Early Transition Metals", Academic Press, New York, 1972, p 351.
(26) H. Schäfer, H. G. von Schnering, J. Tillack, F. Kuhnen, H. Wöhrle, and H. Bauman, *Z. Anorg. Allg. Chem.*, **353**, 281 (1967).
(27) Reference 25, pp 354, 355.
(28) S. Stensvad, B. J. Helland, M. W. Babick, R. A. Jacobson, and R. E. McCarley, *J. Am. Chem. Soc.*, **100**, 6257 (1978).
(29) P. A. Vaughan, J. H. Sturdivant, and L. Pauling, *J. Am. Chem. Soc.*, **72**, 5477 (1950).
(30) R. D. Burbank, *Inorg. Chem.*, **5**, 1491 (1966).
(31) P. B. Fleming, T. A. Dougherty, and R. E. McCarley, *J. Am. Chem. Soc.*, **89**, 159 (1967).
(32) Binding energy data for $(Mo_6Br_8)Br_4$ and its derivatives differ by +1.0 eV from that reported previously in a preliminary communication[12] because of the different referencing procedures used.
(33) These and all other halogen X_b:X_t intensity ratios reported in this paper are within 5% of the integral numbers quoted.
(34) H. D. Glicksman, A. D. Hamer, T. J. Smith, and R. A. Walton, *Inorg. Chem.*, **15**, 2205 (1976).
(35) H. D. Glicksman and R. A. Walton, *Inorg. Chem.*, **17**, 200 (1978).
(36) Pertinent data are as follows: β-$MoBr_2$, Br $3p_{1/2}$ and $3p_{3/2}$ at 188.7 and 182.1 eV (fwhm = 2.3 eV for $3p_{3/2}$ component); β-MoI_2, I $3d_{3/2}$ and $3d_{5/2}$ at 630.8 and 619.3 eV (fwhm = 2.0 eV for the $3d_{5/2}$ component).

Contribution from the Department of Chemistry,
Brown University, Providence, Rhode Island 02912

Electrical and Optical Properties of the System $TiO_{2-x}F_x$

S. N. SUBBARAO, Y. H. YUN, R. KERSHAW, K. DWIGHT, and A. WOLD*

Received July 7, 1978

A convenient method for preparing compounds in the system $TiO_{2-x}F_x$ has been developed. The electronic and photoelectric properties of samples prepared accordingly have been studied. The fluorine content was found to be an essentially linear function of the reaction temperature over the range 575–700 °C. The saturation photocurrent increased with decreasing fluorine content, because of increased response at the longer wavelengths. This improved response may be attributed to the increase in depletion-layer width arising from the observed increase in resistivity. A significantly larger saturation photocurrent was obtained from samples of $TiO_{2-x}F_x$ than from comparable samples of TiO_{2-x} under the same conditions. The increased output may be attributed to a decrease in the recombination rate brought about by the filling of oxygen vacancies. The long-term stability was studied, and a sample of $TiO_{2-x}F_x$ was found to be at least as stable, in a suitable electrolyte, as comparable TiO_{2-x}.

Introduction

In most of the previous studies dealing with oxides which have served as n-type electrodes, increased conductivity was achieved by the production of oxygen deficiencies. Whereas earlier publications on n-type anodes such as TiO_{2-x} indicated that they were stable, there has been recent evidence[1] that these compounds do not show long-term stability in the presence of the production of oxygen at their surfaces. An alternate method of producing conducting electrodes is by the chemical substitution of fluorine for oxygen, rather than the creation of oxygen vacancies. Both methods result in the formation of $3d^1$ titanium, which would account for the relatively high conductivity obtained.

In a recent publication, Derrington et al.[2] reported on the photoelectrolytic behavior of $WO_{3-x}F_x$. It was found that the substitution of fluorine for oxygen in WO_3 did not adversely affect the photoelectric properties of WO_3 but increased the stability of the compound when used as a photoanode. One might expect members of the system $TiO_{2-x}F_x$ also to show increased stability over TiO_{2-x}, since all of the anion sites would be occupied. It is the purpose of this study to prepare members of the series $TiO_{2-x}F_x$ and to determine their photocurrents and stability as photoanodes in photoelectrolysis cells.

Sample Preparation

Wafers 1 mm thick were sliced from a single-crystal boule obtained from National Lead Industries, South Amboy, N.J., using a water-cooled diamond saw. Each wafer was sandblasted in order to produce homogeneous surfaces, cleaned in an ultrasonic bath, and then wrapped in a piece of platinum gauze. The gauze and wafer were inserted into a sleeve made from 0.005 in. thick titanium foil

0020-1669/79/1318-0488$01.00/0

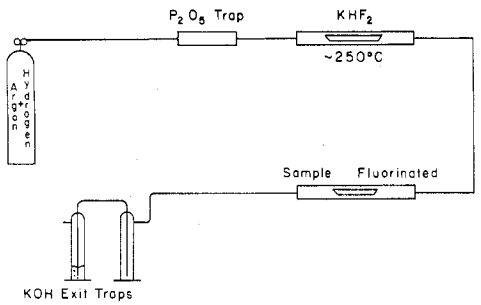

Figure 1. Schematic illustration of the fluorination apparatus.

obtained from MRC Corp., Orangeburg, N.Y. The encapsulated sample was then centered within a nickel boat. This boat was positioned within a nickel tube (the "sample" tube) and centered with respect to the hot zone of one furnace, as illustrated in Figure 1.

Hydrogen fluoride was generated by the thermal decomposition of potassium bifluoride at 260 °C. A nickel boat containing approximately 18 g of potassium bifluoride was positioned within a second nickel tube (the "KHF_2" tube), and centered in the hot zone of a second furnace. Figure 1 depicts the arrangement of the furnaces and gas train used for the preparation of the $TiO_{2-x}F_x$ samples. A gas mixture of 85% argon and 15% hydrogen was dried by passing through a phosphorus pentoxide drying tube, flowed over the potassium bifluoride (which was kept at 260 °C), passed over the sample, and finally exited through a sodium hydroxide bubbler.

The fluorinating system was purged with 85% argon–15% hydrogen gas for about 12 h at room temperature. The sample tube was then positioned in its furnace and both furnaces were turned on. The sample was allowed to heat and equilibrate at the desired reaction temperature for 1 h. The KHF_2 tube was then placed in its furnace, which already had reached the temperature of 260 °C. The generation of hydrogen fluoride began immediately, and the time of the fluorination run started at that moment. Samples were fluorinated at temperatures between 575 and 700 °C. Attempts to fluorinate a TiO_2 wafer at 550 °C failed to yield a homogeneous product. After 8 h of fluorination, the sample furnace was shut off and allowed to cool for 1 h. The tube was removed from the furnace and cooled to room temperature. The exit gas stream was then tested with pH test paper to verify that hydrogen fluoride was still being produced. The KHF_2 tube was removed from its furnace and the sample was taken out of its sleeve.

Samples prepared in this manner appeared pale blue to black. The darker colors resulted from higher temperature preparations. Each sample was subdivided into appropriate pieces for the ensuing measurements by means of a string saw using a silicon carbide slurry.

Thermogravimetric Analysis

Samples of $TiO_{2-x}F_x$ were prepared for analysis by grinding a piece of each fluorinated wafer to give approximately 100 mg of sample. The finely divided powder was heated in an oxygen atmosphere from room temperature to 1000 °C and changes in the weight were recorded using a Cahn electrobalance (Model RG) and a chart recorder. None of the samples in the series showed any measurable weight change, which indicated that within the sensitivity of the balance there were no measurable additional vacancies present in the compounds studied. The extent to which additional vacancies can be determined corresponds to an uncertainty of 0.005 in the value of x.

Fluorine Analysis

Samples of finely divided $TiO_{2-x}F_x$ powder were subjected to pyrosulfate fusion. During the fusion process, a stream of nitrogen gas saturated with water vapor was passed over the melt. The gas stream carried the hydrogen fluoride produced by hydrolysis of the sample into a 1 M solution of sodium hydroxide. The resulting solution was diluted to 50 mL with a buffer solution of potassium acetate and acetic acid. The final pH of the solution was 5.5. The fluoride was determined with an Orion fluoride electrode (Model 94-09). The fluoride content of the sample fluorinated at 700 °C gave a value of x in $TiO_{2-x}F_x$ of 0.002, whereas that of the sample fluorinated at 600 °C gave a value of $x = 0.0001$, which was the limit detectable by the fluoride electrode and is subject to some uncertainty, since the value of x in this material can be reported only within an accuracy equivalent to ±0.0002.

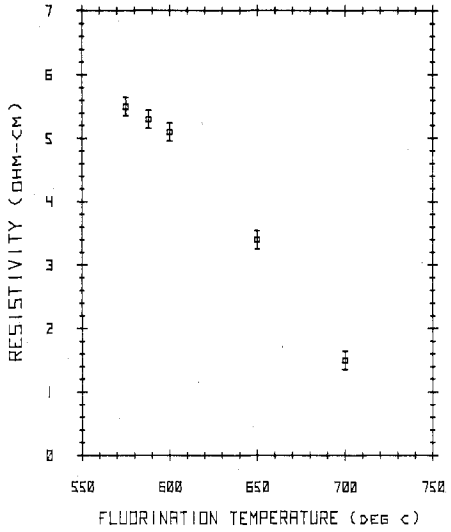

Figure 2. Variation of resistivity with the fluorination temperature of $TiO_{2-x}F_x$ electrodes.

Electrical Properties

A bar approximately 4 × 2 × 1 mm was cut from each of the fluorinated wafers in such a fashion that only the two large faces belonged to the outside surface of the sample. Each bar was further subdivided into three sections 4 × 2 × 0.25 mm in order to establish whether or not each fluorinated wafer was truly homogeneous. Thus the middle section was taken entirely from the interior of the wafer and made no contact with the outside surface. Indium leads were bonded ultrasonically to each section, and the standard Van der Pauw technique[3] was used to measure its resistivity. Excellent agreement, within experimental error, between the resistivity values for inside and outside sections was obtained for all the fluorinated wafers considered in this study. This result demonstrates that the fluorination process had penetrated uniformly throughout each sample. The measured resistivity values are shown as a function of fluorination temperature in Figure 2.

The resistivity of 1.5 Ω cm and fluorine concentration of $x = 0.0020$ (2) determined for samples fluorinated at 700 °C imply an electron mobility of 0.06 (1) $cm^2/(V\ s)$ if each fluorine ion produces a conduction electron. This value is reasonably close to reported mobilities, somewhat dependent upon sample preparation, of about 0.1 $cm^2/(V\ s)$.[4] The assumption that the mobility is independent of fluorine concentration would yield deduced values of $x = 0.000\,89$ (15), 0.000 59 (10), and 0.000 55 (9) for fluorination temperatures of 650, 600, and 575 °C, respectively.

Photoelectric Properties of Fluorinated TiO_2 Anodes

Electrodes were prepared by cutting pieces approximately 4 mm square from the fluorinated samples and evaporating a thin coating of copper onto the back of each to provide good electrical contacts. The high quality of such contacts was verified on test samples both by resistance curve tracing and by agreement between two-probe and four-probe resistivity values to within the accuracy of measurement. Anode assemblies were fabricated by using indium metal to solder these electrodes to platinum wires which had been sealed in small Pyrex tubes and then coating all but the front surface with an electrically insulating resin (Microstop, Michigan Chrome and Chemical Co.). Care was taken not to disturb the active photosurface. For measurement, these anodes were mounted in a small glass cell approximately 8 mm from the quartz

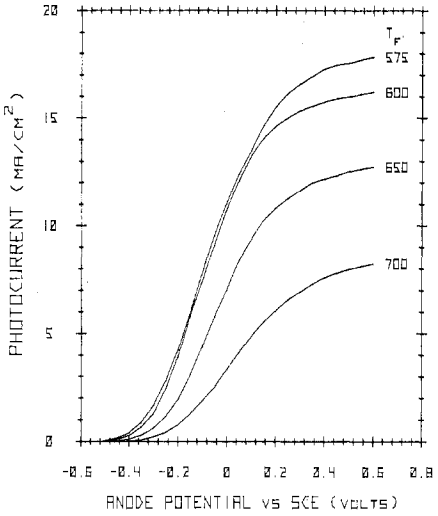

Figure 3. Dependence of photocurrent upon anode potential (SCE reference) for $TiO_{2-x}F_x$ electrodes fluorinated at various temperatures T_F for "white" xenon arc irradiation of 1.25 W/cm².

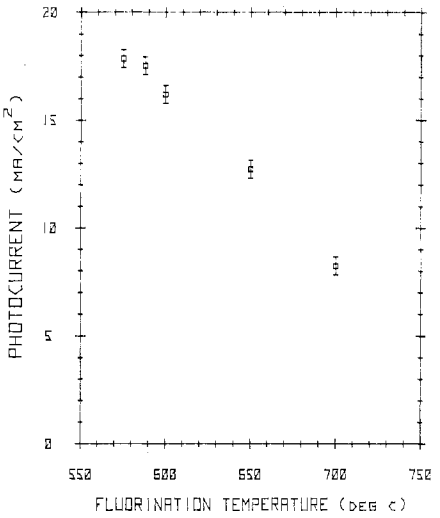

Figure 4. Variation of saturation photocurrent, measured at an anode potential of 0.6 V, with the fluorination temperature of $TiO_{2-x}F_x$ electrodes for "white" xenon arc irradiation of 1.25 W/cm².

window. A platinized platinum cathode (2.5 cm² in area) was mounted 2 cm behind and below the anode and a saturated calomel reference electrode (SCE) 10 cm above it. The cell was filled with 100 mL of 0.2 M sodium acetate electrolyte (pH $\simeq$7.5) which was purged of dissolved oxygen by continuous bubbling of 85% argon–15% hydrogen gas. A cathode potential of approximately −0.64 V vs. SCE was used as the criterion for completed purging.

A 150-W xenon arc was used to illuminate an aperture 5 mm in diameter, which was imaged onto the anode by means of a quartz lens. This resulted in a reproducible area 2.25 mm in diameter irradiated with approximately 50 mW total power. The instantaneous power was determined for each curve by using a calibrated Eppley thermopile (16-junction Coblentz-type). Anodic bias was applied via a voltage follower having an output impedance less than 0.1 Ω, and the resulting photoresponse was measured with a current amplifier which inserted a negligible potential drop (<1 μV) in the external circuit.

The variation of photocurrent with anode potential (measured against SCE) is shown in Figure 3 for samples fluorinated at several temperatures (T_F) between 575 and 700 °C. The indicated photocurrent densities have all been normalized to a total irradiation of 12.5 mW/mm², corresponding to 50 mW incident over the illuminated area of 4 mm². It is evident that the saturation photocurrent (measured at an anode potential of 0.6 V) increases significantly with decreasing fluorination temperature over this range, and the essentially linear nature of this relationship can be seen in Figure 4. The peak photocurrent of 17.9 mA/cm² obtained here is approximately twice the maximum (9.2 mA/cm²) found with unfluorinated TiO_{2-x} under similar conditions.[5]

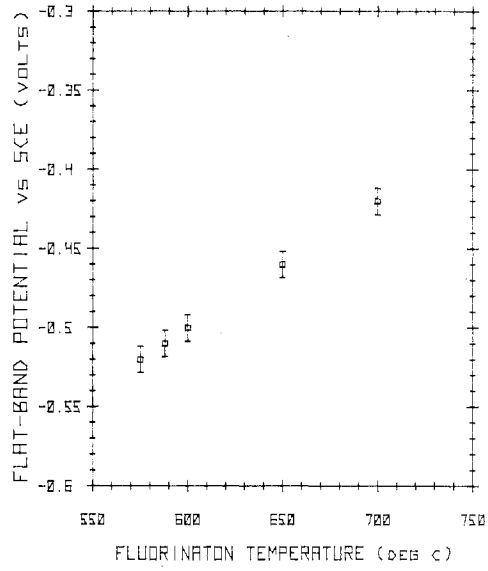

Figure 5. Variation of flat-band potential (SCE reference) with the fluorination temperature of $TiO_{2-x}F_x$ electrodes.

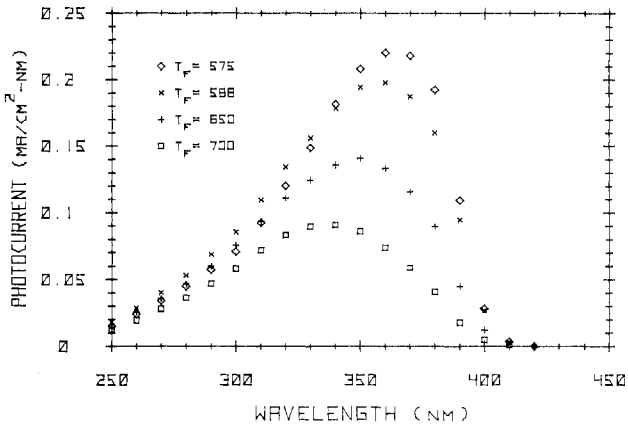

Figure 6. Spectral photoresponse of $TiO_{2-x}F_x$ for electrodes fluorinated at various temperatures T_F, normalized to "white" xenon arc irradiation of 1.25 W/cm².

The lateral shift of the curves presented in Figure 3 results from a systematic variation of the flat-band potential (U_{fb}). Values for U_{fb} (measured against SCE) were obtained from the linear dependence of the square root of the photocurrent upon anode potential for small values of the current (values <0.5 mA/cm² in Figure 3). They are shown plotted against fluorination temperature in Figure 5. The observed increase in flat-band potential corresponds to a decrease in its energy. This decrease in energy appears anomalous for an increase in carrier concentration, which would be expected to raise the Fermi level, but similar behavior has been reported elsewhere.[6] Furthermore, as kindly pointed out by one of the referees, a change in the chemical potential for fluorine ions occurs at the solid–liquid interface, and the resulting potential drop can be expected to increase with increasing fluorine concentration.

The spectral photoresponse of the fluorinated electrodes was studied by inserting an Oriel monochromator (Model 7240) in place of the 5-mm. aperture. The curves shown in Figure 6 were obtained at an anode potential of 0.6 V with a slit width

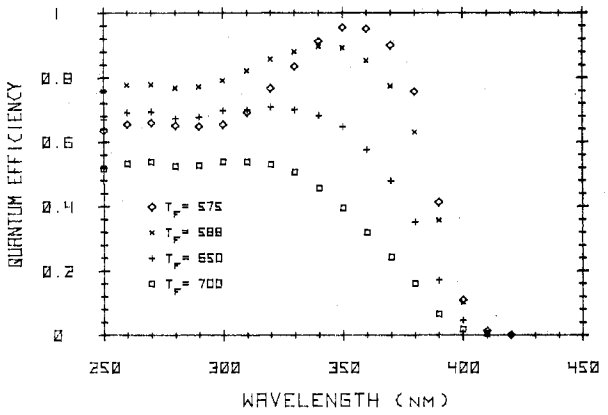

Figure 7. Quantum efficiency in electrons per photon as a function of excitation wavelength for $TiO_{2-x}F_x$ electrodes fluorinated at various temperatures T_F.

of 0.5 mm, which gave a spectral resolution of 4 nm. The photocurrents have been normalized so as to yield integrated outputs corresponding to the values given in Figure 4. These data can also be expressed in terms of quantum efficiency (electrons per photon) by dividing the observed photocurrent (electrons per second) by the incident radiation (photons per second). The curves presented in Figure 7 have not been corrected for any absorption in the electrolyte or cell window nor for reflection from the sample surface. From Figures 6 and 7, it can be seen that the increase in photocurrent observed with decreasing fluorination temperature arises from increased responsivity at the longer wavelengths. These wavelengths penetrate more deeply into the electrodes, and their photogenerated electron-hole pairs will become separated only if this penetration is less than the width of the depletion layer. Thus the improved response observed at low T_F may be attributed to the increase in depletion-layer width resulting from the increase in resistivity seen in Figure 2.

Although the depletion layer must also widen with decreasing conductivity in TiO_{2-x}, no shift in the spectral response is produced.[5] This difference in behavior can only be due to the oxygen vacancies, which can serve as traps and recombination centers. These traps impede the separation of photogenerated electron-hole pairs and promote their recombination. Their effectiveness is greatest where the potential gradient available for charge separation is small, namely, deep in the anode when the depletion layer is wide. Thus they can be expected to quench out the photocurrent which might otherwise arise from longer-wavelength photons as the conductivity decreases, thereby inhibiting any shift in the spectral response.

The maximum photocurrent in the system TiO_{2-x} is obtained by reduction at 600 °C.[5] The spectral photoresponse of such a sample, normalized to 9.2 mA/cm^2 integrated output,[5] is compared with that obtained for optimized $TiO_{2-x}F_x$ in Figure 8. It is evident that the fluorinated material gives an appreciably greater response at the longer wavelengths. The solar spectrum falls off much more rapidly below 400 nm than the xenon-arc spectrum. Thus the disparity between the outputs of fluorinated and reduced rutile would be greatly enhanced under solar irradiation.

In addition, the long-term stability of electrodes prepared from these same two samples has been determined under 125 mW/mm^2 irradiation with an applied anodic bias of 1.5 V. The resulting decay of photocurrent with time is shown in Figure 9. The reduced electrode showed similar behavior in both 0.2 M sodium acetate and 0.2 M K_2SO_4 adjusted to a pH of 7.5. The fluorinated electrode was found to be appreciably less stable than the reduced electrode in 0.2 M sodium acetate, presumably because of hydrolysis of the

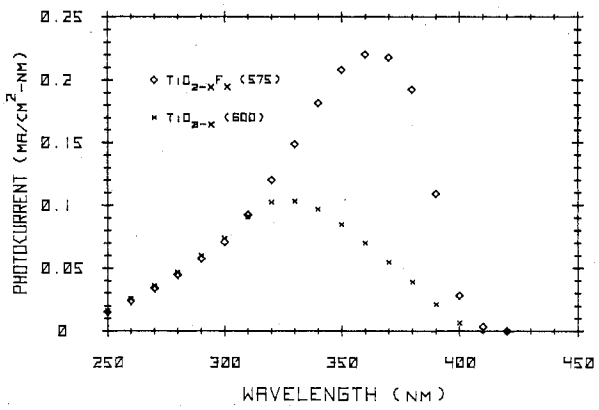

Figure 8. Comparison between the spectral photoresponse of $TiO_{2-x}F_x$ electrodes fluorinated at 575 °C and that of TiO_{2-x} electrodes reduced at 600 °C, normalized to "white" xenon arc irradiation of 1.25 W/cm^2.

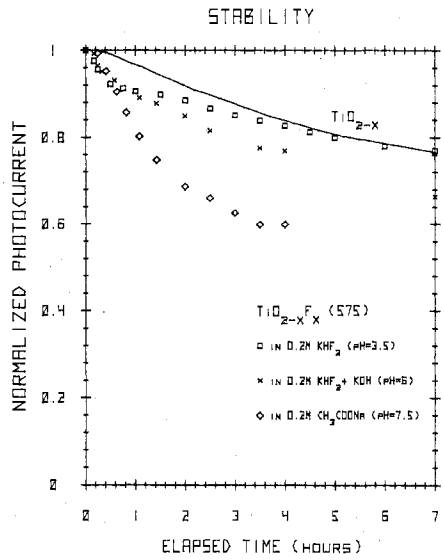

Figure 9. Comparison between the decay of photocurrent with time for TiO_{2-x} electrodes in 0.2 M sodium acetate and that for $TiO_{2-x}F_x$ electrodes fluorinated at 575 °C in 0.2 M potassium bifluoride, 0.2 M potassium bifluoride buffered with potassium hydroxide, and 0.2 M sodium acetate. Measurements were made with 1.5 V of anodic bias under "white" xenon arc irradiation of 1.25 W/cm^2.

fluoride ions. Such hydrolysis should be suppressed by a sufficient concentration of fluoride ions in the electrolyte. Measurements were made in a Lucite cell having a fluorite window 2 mm thick with a 0.2 M solution of potassium bifluoride buffered to a pH of 6 with potassium hydroxide and with a 0.2 M solution of unbuffered potassium bifluoride (pH 3.5). As seen in Figure 9, the hydrolysis was partially and completely suppressed, respectively, by these two electrolytes. In the latter case, the long-term stability was improved over that of unfluorinated rutile.

Summary and Conclusions

A procedure for the fluorination of 1 mm thick wafers of rutile has been developed. The resulting products $TiO_{2-x}F_x$ were found to contain fluorine by chemical analysis, to be stoichiometric by thermogravimetric analysis, and to be homogeneous by resistivity analysis. The value of x was found to be an essentially linear function of the fluorination temperature over the range 575–700 °C from measurements of the resistivity, saturation photocurrent, and flat band potential. Analysis gave the value $x = 0.002$ for preparation at 700 °C.

Samples with the smallest value of x showed the largest photocurrent, despite their having the highest resistance. Most of the variation of photocurrent with x occurred in the

long-wavelength part of the spectrum, and hence was attributed to variation of the depletion-layer width with carrier concentration.

Under irradiation from a xenon arc source, rutile wafers fluorinated at 575 °C produced almost twice the photocurrent obtained from rutile reduced at the optimum temperature (600 °C). The long-wavelength photoresponse was significantly enhanced in the fluorinated material, presumably by the filling of the oxygen vacancies. This enhancement would become appreciably more pronounced under solar irradiation, which provides considerably less relative power at wavelengths below 350 nm.

The long-term stability of fluorinated electrodes in a suitable electrolyte under conditions of intense irradiation and extreme anodic bias was found to be at least as good as that of an optimally reduced electrode. Hydrolysis of the electrodes was completely suppressed by maintaining an adequate concentration of fluoride ions in the aqueous electrolyte. Furthermore, it should be noted that the fluorinated material produced a higher photocurrent than the reduced electrode even after 4 h of operation in the sodium acetate solution. Thus it appears that definite improvement over the photoelectric efficiency of reduced rutile electrodes can be achieved by fluorination.

Acknowledgment. The office of Naval Research, Arlington, Va., supported the work of S.N.S. and K.D. Acknowledgment is made to the National Science Foundation for the support of Y.H.Y. In addition, the authors would like to acknowledge the support of the Materials Research Laboratory Program at Brown University. The authors also wish to express their support to Dr. W. Godek for his assistance with the development of a method for fluorine analysis.

Registry No. TiO_2, 13463-67-7; fluorine, 7782-41-4.

References and Notes

(1) L. A. Harris and R. H. Wilson, *J. Electrochem. Soc.*, **123**, 1010 (1976); L. A. Harris, D. R. Cross, and M. E. Gerstner, *ibid.*, **124**, 839 (1977).
(2) C. E. Derrington, W. S. Godek, C. A. Castro, and A. Wold, *Inorg. Chem.*, **17**, 977 (1978).
(3) L. J. Van der Pauw, *Phillips Tech. Rev.*, **20**, 220 (1958).
(4) G. A. Acket and J. Volger, *Phys. Lett.*, **8**, 244 (1964); V. N. Bogomolov and V. P. Zhuze, *Sov. Phys.—Solid State (Engl. Transl.)*, **8**, 1904 (1967).
(5) S. N. Subbarao, Y. H. Yun, R. Kershaw, K. Dwight, and A. Wold, to be submitted for publication.
(6) J. F. Dewald, *J. Phys. Chem. Solids*, **14**, 155 (1960).

Contribution from the Departments of Chemistry, Howard University, Washington, D.C., and University of Virginia, Charlottesville, Virginia 22901

Magnetic Properties of Some Monomeric and Dimeric Nickel(II) Complexes $NiLX_2$ (L = 2,9-Dimethyl-1,10-phenanthroline (dmp), 2,2′-Biquinolyl, Bathocuproine; X = Cl, Br, I) and the Crystal Structure of $Ni(dmp)I_2$

RAY J. BUTCHER, CHARLES J. O'CONNOR, and EKK SINN*

Received August 31, 1978

The magnetic properties of a series of nickel(II) complexes with the empirical formula $NiLX_2$ are reported and analyzed in terms of their molecular structures. Here L = 2,9-dimethyl-1,10-phenanthroline (dmp), 2,2′-biquinolyl (biq), or 2,9-dimethyl-4,7-diphenylphenanthroline (bathocuproine, bc) and X = Cl, Br, or I. Some of the complexes are known to be dimeric, some monomeric, and $Ni(dmp)I_2$ is shown to be monomeric by crystal X-ray diffraction. Two of the dimeric complexes, $[Ni(biq)Cl_2]_2$ and $[Ni(dmp)Cl_2]_2$, show significant intramolecular antiferromagnetic interactions, two less strongly linked dimers, $[Ni(bc)Cl_2]_2$ and $[Ni(dmp)Br_2]_2$, show weaker antiferromagnetism, and one probable dimer, $[Ni(bc)Br_2]_2$, is weakly antiferromagnetic. The pseudotetrahedral monomeric complexes $Ni(biq)Br_2$, $Ni(biq)I_2$, $Ni(dmp)I_2$, and $Ni(bc)I_2$ have magnetic properties which qualitatively resemble the weakly antiferromagnetic dimers and are analyzed in terms of spin–orbit coupling. Crystal data for $Ni(dmp)I_2$: $NiI_2N_2C_{14}H_{12}$, space group $P2_1/n$, a = 8.472 (2) Å, b = 14.248 (3) Å, c = 13.516 (3) Å, β = 102.72 (2)°, V = 1591 Å^3, R = 3.5%, 2632 reflections.

Introduction

Magnetic and chemical interactions between dimeric metal complexes have been an area of long-standing interest.[1] Recently the preparation and crystal structure has been reported[2] for a series of nickel(II) compounds of the empirical formula $NiLX_2$. The compounds previously reported are shown to produce dimeric and single monomeric units depending on the ligand or anion. The ligand L may be biquinoline (biq), dimethylphenanthroline (dmp), or bathocuproine (bc); the anion X may be Cl, Br, or I. Another of the structures is reported here along with a detailed analysis of the magnetic properties of each member of the series.

The compounds are most easily studied when grouped as monomers or dimers. All of the chlorides form the dimeric complexes $[NiLCl_2]_2$ with five-coordinate nickel ions and two bridging chlorines. The iodides form the monomeric complexes $NiLI_2$, with the coordination sphere of the nickel ion having distorted tetrahedral symmetry. The bromides occupy the middle ground with $Ni(biq)Br_2$ being monomeric and $[Ni(dmp)Br_2]_2$ and $[Ni(bc)Br_2]_2$ having the dimeric form.

The magnetic properties of $[Ni(dmp)Cl_2]_2$ have been reported previously.[3] Our results agree qualitatively regarding the antiferromagnetic dimeric interactions; however quantitative differences in the data exist (i.e., position and height of the maximum of the susceptibility).

The compounds are analyzed in terms of dimeric or monomeric magnetic theory as required by the symmetry from the crystallographic data, and the crystal structure of the pseudotetrahedral complex (2,9-dimethyl-1,10-phenanthroline)diiodonickel(II), $Ni(dmp)I_2$, is reported.

Experimental Section

Preparation. Both the dimeric and monomeric compounds were prepared by the same method. The nickel halide was dissolved in triethyl orthoformate, and the ligand was dissolved in benzene. The compounds precipitated on mixing the two solutions; they were then recrystallized from nitrobenzene, and crystals suitable for X-ray analysis were obtained.

Magnetic Susceptibility. The magnetic susceptibility was recorded with a superconducting susceptometer[4] in the 4–100 K temperature region. All compounds were measured as powder samples and at fields ranging from 80 to 400 Oe.

Crystal data for (2,9-dimethyl-1,10-phenanthroline)diiodonickel(II), $Ni(dmp)I_2$: $NiI_2N_2C_{14}H_{12}$, yellow-brown crystal, space group $P2_1/n$, a = 8.472 (1) Å, b = 14.248 (3) Å, c = 13.516 (3) Å, β = 102.72 (2)°, V = 1591 Å^3, μ(Mo Kα) = 51.4 cm^{-1}, ρ_{calcd} = 2.18 g cm^{-3}, ρ_{obsd} = 2.21 g cm^{-3}; crystal dimensions (mm from centroid), (110) 0.16, ($\bar{1}\bar{1}$0) 0.16, (1$\bar{1}$0) 0.16, ($\bar{1}$10) 0.16, (011) 0.19, (0$\bar{1}\bar{1}$) 0.19, (01$\bar{1}$) 0.17, (0$\bar{1}$1) 0.17, (10$\bar{1}$) 0.32, ($\bar{1}$01) 0.32; maximum and minimum transmission coefficients are 0.42 and 0.30, respectively.

0020-1669/79/1318-0492$01.00/0